Supracrustal input to magmas in the deep crust of Sierra Nevada batholith: Evidence from high-δ^{18}O zircon

Jade Star Lackey[a],*, John W. Valley[a], Jason B. Saleeby[b]

[a]Department of Geology and Geophysics, University of Wisconsin, Madison, WI 53706, United States
[b]Division of Geological and Planetary Sciences, California Institute of Technology, Pasadena, CA 91125, United States

Abstract

Oxygen isotope ratios of zircon (Zc) from intrusives exposed in the Tehachapi Mountains, southern California, reveal large inputs of high-δ^{18}O supracrustal contaminant into gabbroic and tonalitic magmas deep (>30 km) in the Cretaceous Sierra Nevada batholith. High δ^{18}O(Zc) values (7.8 ± 0.7‰) predominate in the deep parts of the batholith, but lower values (6.1 ± 0.9‰) occur in shallower parts. This indicates a larger gradient in δ^{18}O with depth in the batholith than occurs from west to east across it. Oxygen, Sr, and Nd isotope data show that the supracrustal contaminant was likely young (Paleozoic or Mesozoic), hydrothermally altered upper oceanic crust or volcanic arc sediments. Such rocks were subducted or underthrust beneath the Sierran arc during accretion of oceanic terranes onto North America. This component yielded high-δ^{18}O magmas that were added to the base of the batholith. On average, gabbros in the southern Sierra contain at least 18% of the subducted supracrustal component. Some tonalite and granodiorite magmas were additionally contaminated by Kings Sequence metasedimentary rocks, as evidenced by δ^{18}O(Zc) and initial ^{87}Sr/^{86}Sr that trend toward values measured for the Kings Sequence. Besides high δ^{18}O values in the southern Sierra, xenoliths in the central Sierra also have elevated δ^{18}O, which confirms the widespread abundance of supracrustal material in the sub-arc lithospheric mantle. In contrast to δ^{18}O(Zc), whole rock δ^{18}O values of many samples have undergone post-magmatic alteration that obscures the magmatic contamination history of those rocks. Such alteration previously prevented confident determination of the mass of young, hydrothermally altered mantle rocks that contributed to Sierran granitoids.
© 2005 Elsevier B.V. All rights reserved.

Keywords: oxygen isotopes; zircon; granitoids; alteration; Sierra Nevada; Tehachapi Mountains

1. Introduction

Understanding convergent margin magmatism is essential to unraveling processes of crustal growth and maturation. Granitic batholiths at continental con-

* Corresponding author. Tel.: +1 608 263 3453.
  E-mail address: jadestar@geology.wisc.edu (J.S. Lackey).

vergent margins are thought to represent crust generated by interaction of mantle-derived magmas and pre-existing continental crust. Studies of continental margin batholiths have sought to understand how

mantle and crustal components interact at different depths, and how much material is added versus recycled (e.g., [1–3]). A particularly important but elusive parameter of magma generation at convergent
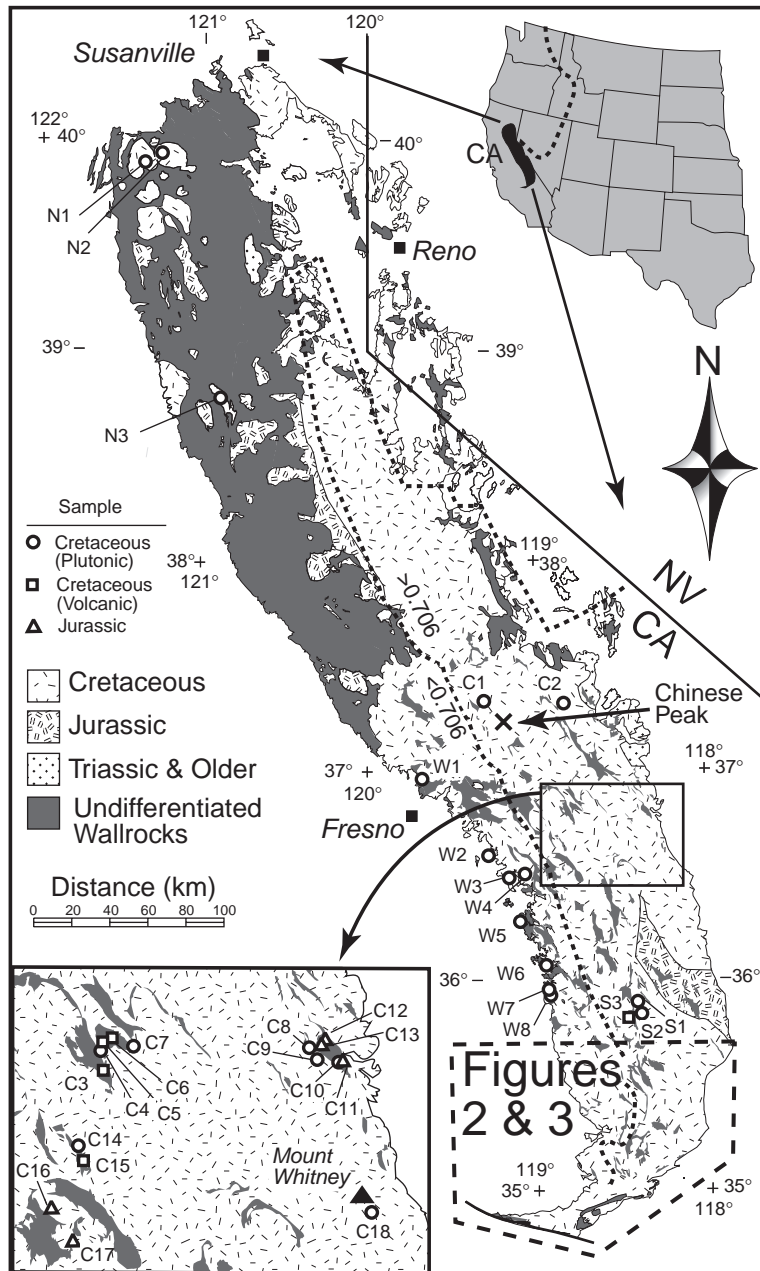

Fig. 1. Generalized geologic map of the Sierra Nevada batholith. Sample locations are indicated for rocks studied in the northern, western and central Sierra Nevada. Sr$_i$ = 0.706 isopleth [4] is shown for reference. Map after Jennings et al. [5] and Moore and Sisson [6].

margin batholiths regards knowing the mass of young (relative to the batholith's age), mantle-derived rock that is remelted and recycled. Knowing this parameter is critical to understanding heat balance, cooling rates, and volatile budgets (e.g., CO_2), which are factors that in turn affect processes of deformation, as well as ore formation.

The Mesozoic Sierra Nevada batholith (SNB) in California (Fig. 1) is one of the best studied convergent margin batholiths. Excellent exposures and a wealth of existing data make the SNB an ideal location to study crustal growth and recycling processes. Considerable uncertainty remains, however, as to the sources and amounts of different crustal and mantle "reservoirs" and the mechanisms by which they were incorporated into Sierran magmas. Three reservoirs generally thought to have influenced magma chemistry in the Sierran arc are: 1) craton-derived sedimentary rocks; 2) ancient lower continental crust, and 3)

young depleted mantle. The location and relative abundance of these reservoirs in the crustal cross-section of the arc, especially at its deepest levels, remain speculative and controversial.

Oxygen isotopes help fingerprint different reservoirs. They are particularly well suited for identifying recycling of young, supracrustal (volcanic) rocks in convergent margin arcs because $\delta^{18}O$ values in these rocks are often reset by hydrothermal alteration, soon after they crystallize. In contrast, radiogenic isotopes are not modified considerably by hydrothermal alteration [7], and they can only identify recycled material that is sufficiently old to have undergone ingrowth of radioactive decay products. Consequently, in young mantle-derived rocks, like altered ocean crust, $\delta^{18}O$ values are often significantly shifted from mantle values, whereas changes of Sr isotope ratio are minimal, and Nd and Pb isotope ratios are essentially unchanged [7]. Thus, in arc settings, oxygen isotopes
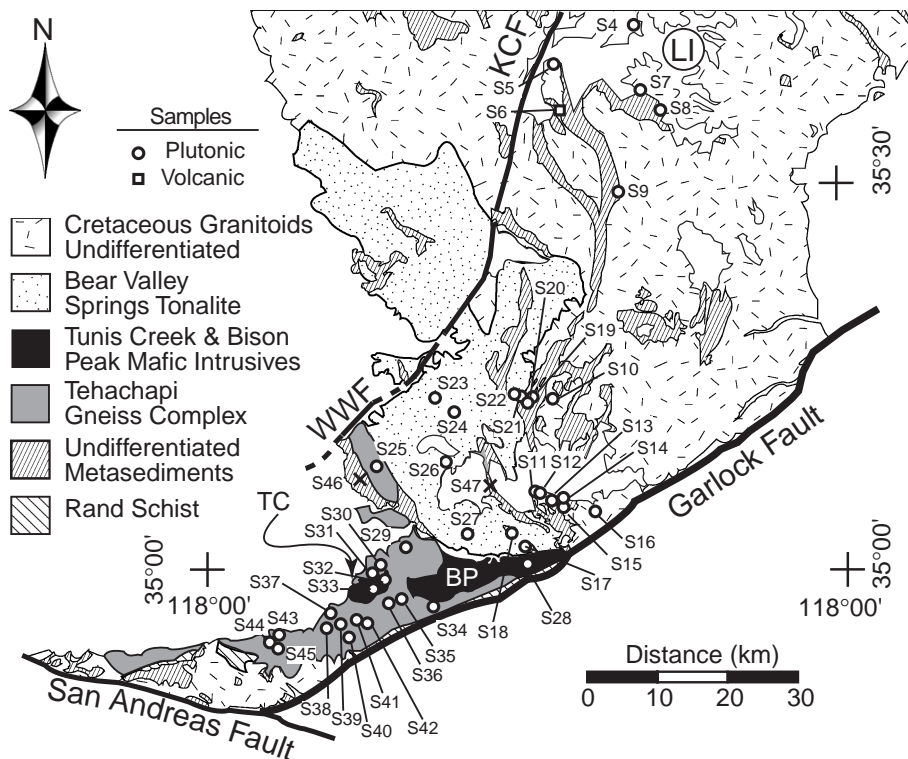

Fig. 2. Geology of the southern Sierra, including the Tehachapi Gneiss complex and Bear Valley Springs intrusive suite. Metasedimentary rocks are predominantly from the Kings Sequence. WWF=White Wolf Fault; KCF=Kern Canyon Fault; LI=Lake Isabella; TC=Tunis Creek Gabbro; BP=Bison Peak tonalite; after Wood and Saleeby [12].

are unique monitors for recycling of young, mantle-derived rock that resided near earth's surface, and they can provide a quantitative estimate of such recycling. Furthermore, the interpretation of mass balance calculations is simplified by the fact that oxygen is a major element in most rocks.

Taylor and Silver used oxygen isotopes to detect recycling of supracrustal rocks in a classic study of the Peninsular Ranges batholith of southern California [8]. There, correlation of whole rock (WR) $\delta^{18}O$ and initial $^{87}Sr/^{86}Sr$ (Sr_i) revealed variable input of altered ocean crust to magmas across the batholith [8]. A similar study in the SNB [9] showed no clear trend of $\delta^{18}O(WR)$ with respect to trends in the spatial and temporal distribution of radiogenic isotope ratios. From these results, it was concluded that many $\delta^{18}O(WR)$ values were reset by extensive hydrothermal alteration.

In this study, we present analyses of $\delta^{18}O$ made by laser fluorination, from aliquots of zircon (Zc) concentrates previously analyzed by U–Pb methods (e.g., [10,11] and see Appendix A) to date igneous rocks in the SNB (Figs. 1 and 2). Zircons were analyzed because they are highly retentive of magmatic $\delta^{18}O$ values and have been shown to preserve those values better than other minerals, even through hydrothermal alteration and protracted high-temperature metamorphism [13]. The hardiness of zircon is key to studying high pressure igneous rocks of the

Fig. 3. Inferred paleopressure map for the southern Sierra Nevada. Pressures were determined primarily from igneous barometry and metamorphic phase equilibria. After Wood and Saleeby [12].

southern Sierra (Figs. 2 and 3), which have been intensely deformed [12] and altered, as shown by $\delta^{18}O(WR)$ and $\delta D(WR)$ studies there and in the adjacent Mojave Desert [9,14]. Accordingly, analyzing $\delta^{18}O$ of zircon in the southern Sierra allows insight into the record of magmatic processes deep in the batholith that was otherwise obscured by post-magmatic alteration.

2. Geologic background

The Cretaceous part of the SNB represents a large crustal mass with pronounced spatial variation in composition, age, and isotopic chemistry. The exposed granitic batholith, approximately 35,000 km² (Fig. 1), represents at least 1,000,000 km³ of granitic crust formed largely over 35 million years. On the west side of the batholith, plutons are more mafic (gabbros, tonalites, diorites, and quartz diorites); they progressively become more felsic (granodiorites and granites) to the east [15,16]. The changes of lithology correlate to decreasing ages of the rock [17–20] from west (Early Cretaceous) to east (Late Cretaceous) and have also been shown to be accompanied by extreme gradients in major and trace element geochemistry [16,21] as well as in radiogenic isotopes of Sr [4,22], Nd [23], and Pb [24]. The lateral variations of batholith chemistry reflects a transition from accreted Phanerozoic (oceanic) rocks in the western Sierra, to Proterozoic continental lithosphere in the eastern Sierra [4], but also heterogeneity in the pre-batholithic lithospheric mantle beneath the batholith [25].

The depth of exposure throughout most of the Sierra Nevada batholith is 7–13 km (2–4 kbar) [26,27]. In the southern sierra, however, there is a continuous southward deepening gradient between 10–17 km (3–5 kbar) rocks in the Lake Isabella region to 23–30 km (7–9 kbar) rocks in the Tehachapi Mts. (Fig. 3, [26–29]). This gradient has rendered an oblique crustal section through the southern end of the batholith [30,31]. The oblique section was exposed by tectonic uplift and extensional denudation in conjunction with the Late Cretaceous underthrusting of the Rand schist beneath the southernmost Sierra (Fig. 2; [32]). The Tehachapi Mts. exposures allow study of the magmatic processes at and below the base of the granitic portion of the batholith. The exposures include parts of the transition
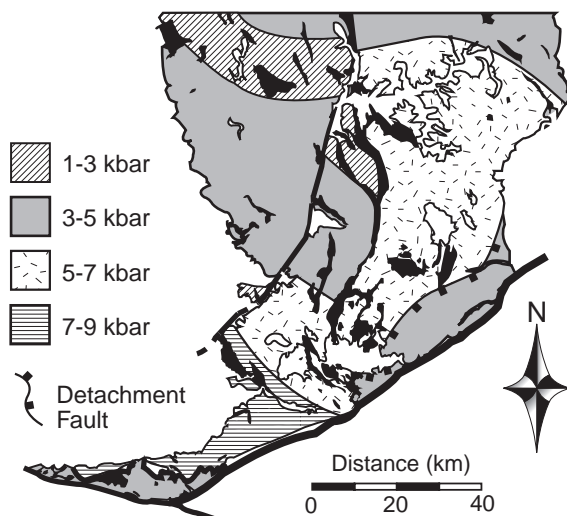
from granitic to underlying mafic cumulate zone, at ~35 km depth, which defined the seismic Moho of the SNB in the Cretaceous [31]. The transition from granitic to cumulate rocks also corresponds to the upper boundary of a MASH (melting, assimilation, storage, and homogenization, e.g., [33]) zone in the lithospheric mantle beneath the SNB [31,34]. In the MASH zone, conditions were favorable for hornblende breakdown and high volume dehydration partial melting of pre-existing lower crustal rocks. Homogenized magmas generated in the MASH zone were then emplaced in the middle and upper crust of the batholith.

High-pressure rocks in the Tehachapi Mts. are divided into two groups that are lithologically and temporally distinct (Fig. 2). The first and oldest group is the Tehachapi Gneiss complex, which contains tonalitic and dioritic gneisses (120 to 110 Ma), plus minor paragneiss bodies. Igneous gneisses in the complex underwent granulite facies metamorphism manifested by garnet growth at the expense of hornblende [11,28,35]. Group two is the 102–97 Ma Bear Valley Springs (BVS) intrusive suite and contains three sub units: (1) the gabbro of Tunis Creek (~102 Ma); (2) the hypersthene tonalite of Bison Peak (~102 Ma); and (3) the tonalite of Bear Valley Springs (~100 ± 2 Ma), including the tonalite of Mt. Adelaide. The BVS rocks are increasingly evolved from the Tunis Creek (~45% SiO_2), to Bison Peak (~60% SiO_2) to the Bear Valley Springs (65% SiO_2) units. Contact relationships between the gneiss complex and the BVS suite are often gradational and have been transposed by ductile flow.

Other southern Sierra igneous rocks occurring east and north of the BVS suite, including those near Lake Isabella, are Mid- to Late Cretaceous (100 to 90 Ma) granodiorites and granites. Locally, these magmas were contaminated (e.g., the granodiorite of Claraville; S10, Fig. 2) by the Kings Sequence [10,36,37].

Patterns of zircon inheritance in the southern Sierra, recorded as U/Pb age discordance, plus Sr and Nd isotope ratios, record progressive contamination of Tehachapi Mts. rock by the Proterozoic crust and sedimentary rocks [10]. For example, only the smallest zircons of the Tunis Creek gabbro have evidence of inherited Proterozoic zircon, suggesting minor late-stage contamination. In the BVS suite, younger and shallower marginal phases and dikes of

the Bear Valley Springs tonalite, including the granodiorite of Claraville, have significant inheritance. Initial Sr and Nd isotope ratios become progressively more radiogenic in younger rocks and essentially track patterns of U/Pb inheritance and demonstrate progressive contamination [10,11].

Collectively, field, petrologic, and geochemical and isotopic studies of the southern Sierra indicate that magmas there are variably contaminated, and that much of the deep, pre-batholithic crust was recycled in the MASH zone of the batholith [31]. The oldest, high-pressure rocks in the Tehachapi Mts. (Figs. 2 and 3) are representative of the magmas produced in the MASH zone of the batholith. However, Sr and Nd isotope compositions in these rocks are inconsistent with recycling of large amounts of Proterozoic pre-batholithic rock [11]. Field and isotopic evidence in shallower rocks near Lake Isabella (Figs. 2 and 3) is consistent with contamination by metamorphic wall-rocks with Proterozoic isotopic compositions, but this superimposed contamination is modest.

3. Sample selection, preparation, and analysis

Sampling focused on rocks of the southern Sierra oblique crustal section that crystallized at 5 to 9 kbar conditions (Figs. 2 and 3). This is thought to proxy for a vertical transect through batholithic rocks which ascended directly from their source regime with little crustal assimilation to medial levels where modest degrees of assimilation are recorded by geologic observations and geochemical data. For comparison, we analyzed representative suites of zircon from the western foothills, northern, and central Sierra (Fig. 1) to determine how $\delta^{18}O(Zc)$ varies regionally in the expansive, shallow to medial level, exposures (1–4 kbar). Many of the Southern SNB samples were previously analyzed for $\delta^{18}O(WR)$, Rb–Sr, and Sm–Nd isotopes [10,11]; Sr_i, and initial $^{143}Nd/^{144}Nd$ (ϵNd) values are calculated from U–Pb zircon ages. Values of $\delta^{18}O(Zc)$ have not previously been measured and can be directly compared to zircon U/Pb ages (which range from 81 to 167 Ma, but most are Cretaceous; see Table 1).

Because the zircons in this study were previously analyzed for U–Pb geochronology, considerable information is already published regarding grain size and

Table 1
δ^{18}O of zircon (‰ VSMOW) in the Sierra Nevada batholith

Sample	Lithology	Age (Ma)	Grain diameter (μm)	δ^{18}O	1 S.D.	$n=$	Sample	Lithology	Age (Ma)	Grain diameter (μm)	δ^{18}O	1 S.D.	$n=$
Western foothills							*Southern Sierra: East Tehachapis, Lake Isabella*						
W1	Tonalite	134	45–62	5.15	0.04	2	S1	Granite	83	45–80	7.95	0.09	2
W2	Gabbro	120	74–149	5.64	0.04	2	"	"		80–120	7.92	0.00	2
W3	Gabbro	110	<45	5.47	0.00	2	S2	Granite	85	60–100	8.21	0.06	1
W4	Tonalite	123	120–165	6.29	0.04	2	S3	Rhyolite	101	45–62	7.94	0.03	2
W5	Granodiorite	120	<44	5.60	0.02	2	S4	Granodiorite	98	45–80	7.80	0.09	2
"	"		44–74	5.70	0.04	2	S5	Granite	90	48–80	7.66	0.01	2
W6	Granodiorite	118	74–149	5.58	0.01	2	S6	Rhyolite	105	45–80	8.50	0.07	2
W7	Gabbro	115	<44	6.76	0.00	2	S7	Granite	98	45–80	8.88	0.00	2
W8	Quartz Diorite	102	44–74	6.17	0.09	2	S8	Granite	100	45–80	9.21	0.02	2
							S9	Granite	95	62–80	8.18	0.01	2
Central and High Sierra							S11	Quartz Diorite	93	62–80	8.56	0.02	2
C1	Granite	99	45–62	6.66	0.00	2	S12	Granite	81	120–165	9.06	0.00	2
"	"		62–80	6.80	0.00	2	S13	Tonalite	95	120–165	8.61	0.04	2
C2	Granodiorite	88	80–100	5.99	0.09	3	S14	Tonalite	96	120–165	9.54	0.04	2
C3	Dacite	105	45–62	7.74	0.05	2	S15	Gabbro	105	120–165	7.77	0.04	2
C4	Granodiorite	102	60–80	7.38	0.04	2	S16	Granodiorite	90	62–80	7.91	0.02	2
C5	Rhyolite	106	45–80	7.32	0.01	2	S17	Granodiorite	97	62–80	7.95	0.06	2
"	"		80–120	7.39	0.02	2	S18	Tonalite	101	62–80	7.99	0.00	2
C6	Dacite	102	45–80	5.55	0.01	2							
C7	Granite	103	45–80	7.41	0.00	2	*Southern Sierra: Tehachapi Gneiss complex*						
C8	Granite	105	45–80	4.97	0.07	2	S20	Granodiorite	117	80–120	7.90	0.02	2
C9	Granodiorite	102	45–80	5.07	0.02	2	S25	Tonalite	115	>120	7.67	0.00	2
"	"		80–120	4.79	0.02	2	S29	Tonalite	117	80–120	7.85	0.02	2
C10	Granite	105	45–80	5.40	0.01	2	S30	Tonalite	115	120–165	6.77	0.00	2
C11	Rhyolite	164	45–80	6.41	0.02	2	S31	Diorite	115	120–165	6.78	0.03	2
C12	Rhyolite	165	62–100	6.34	0.04	2	S34	Tonalite	113	>120	7.43	0.02	2
C13	Rhyolite	167	62–100	6.33	0.02	2	S35	Granite	117	80–120	7.89	0.00	2
C14	Rhyolite	105	62–80	7.21	0.03	2	S36	Tonalite	113	45–80	6.32	0.02	2
C15	Tonalite	115	80–100	5.70	0.11	2	S37	Granite	114	120–165	7.92	0.02	2
C16	Quartz Diorite	162	45–62	5.81	0.01	2	S38	Granite	113	120–165	8.03	0.00	2
C17	Rhyolite	105	62–80	7.34	0.04	2	S39	Tonalite	117	120–165	6.99	0.02	2
C18	Granodiorite	84	<45	5.67	0.01	3	S40	Granite	115	80–120	7.88	0.00	2
							S41	Granite	110	80–120	7.79	0.02	2
							S42	Tonalite	112	80–120	7.90	0.02	2
Southern Sierra: Bear Valley Springs suite							S43	Tonalite	115	80–120	6.63	0.01	2
S10	Granodiorite	90	45–80	9.41	0.02	2	S44	Tonalite	101	45–62	7.45	0.02	2
S19	Tonalite	97	80–120	8.42	0.02	2	S45	Diorite	105	45–62	6.67	0.06	2
S21	Tonalite	98	120–165	7.36	0.01	2	"	"		>120	6.90	0.05	2
S22	Tonalite	97	120–165	7.37	0.00	2	S46	Paragneiss	1460	45–80	11.32	0.00	2
S23	Tonalite	101	120–165	7.28	0.05	1	S47	Quartzite	1708	45–80	11.63	0.02	2
"	"		80–120	7.29	0.05	1							
S24	Quartz Diorite	100	80–120	7.71	0.01	2	*Northern Sierra*						
S26	Tonalite	100	120–165	7.83	0.05	1	N1	Granodiorite	140	45–80	6.00	0.02	2
"	"		45–80	7.78	0.05	1	"	"		80–120	6.16	0.05	1
S27	Tonalite	100	120–165	7.77	0.02	2	N2	Granodiorite	140	45–80	5.90	0.01	2
S28	Tonalite	102	120–165	7.15	0.01	2	"	"		80–120	5.68	0.07	2
S32	Gabbro	102	120–165	7.11	0.01	2	N3	Granodiorite	143	45–62	4.75	0.10	2
S33	Gabbro	102	80–120	6.98	0.03	2	"	"		62–80	4.84	0.04	2

shape, U and Pb isotopic variability, patterns of inheritance and Pb loss and/or U gain [10]. In general, zircons display sizes, shapes, and textures typical of igneous plutonic rocks. Inheritance in zircon can drastically affect U/Pb zircon ages. Oxygen, however, is ~50 wt.% of zircon and thus minor amounts of inherited zircon do not markedly shift the $\delta^{18}O$ value of host zircons. From a mass balance perspective, if a population of zircon and cores inherited therein contrasted in $\delta^{18}O$ by 3‰, the effect of 5 wt.% cores on the resultant $\delta^{18}O$ of the sample would be minimal (~0.15‰). Thus a sample with 5 vol.% inheritance, which can look like much more in a two-dimensional thin section, is not seriously affected in $\delta^{18}O$. Furthermore, samples containing inherited cores were identified in the previous geochronology studies and were avoided in this study, except for two samples of detrital zircons separated from a paragneiss and quartzite (Table 1).

Values of $\delta^{18}O$ were also measured on several mantle xenoliths collected at Chinese Peak, in the central SNB (Fig. 1). The xenoliths are entrained in Miocene trachybasalts and represent fragments of the "root" of residual, melt-depleted rocks, produced during magma generation beneath the Sierran Arc [34]. Xenoliths from levels deeper than the present exposures in the SNB provide important constraints on the vertical $\delta^{18}O$ composition of the batholith.

Zircon was separated by standard crushing and density separation techniques. Least magnetic fractions were concentrated with a Frantz separator as described by Saleeby et al. [10]. Zircon separates were leached with nitric acid, to dissolve non-magnetic phosphate and sulfide minerals, and hydrofluoric acid, which dissolves radiation damaged domains in zircon that are subject to post-magmatic oxygen isotope exchange [13]. Zircon separates were purified by hand-picking under a binocular microscope. Zircon grains were powdered with a boron-carbide mortar and pestle to limit grain size effects and maximize fluorination efficiency. For xenolith analysis, a representative fragment was lightly crushed, and treated with dilute hydrochloric acid to remove grain boundary alteration; individual minerals were then hand-picked to assure purity. The $\delta^{18}O$ of each major phase in a xenolith, and its modal abundance was used to calculate a $\delta^{18}O(WR)$ value (Table 1).

Oxygen isotope analyses were performed in the University of Wisconsin stable isotope laboratory by CO_2 laser fluorination as described by Valley et al. [38]; isotope ratios were measured on a gas source Finnigan MAT 251 mass spectrometer. Analyses were standardized daily by four or more analyses of UWG-2, Gore Mountain garnet standard. Sample $\delta^{18}O$ values were corrected to the accepted value of 5.80‰ for UWG-2 [38]. The average $\delta^{18}O$ of the UWG-2 for 7 days of analyses was 5.72 ± 0.13‰ (day-to-day average $= 5.71 \pm 0.07$‰; standard error $(1 \text{ S.D.}/(n^{0.5}) = \pm 0.03, n = 26)$; the average daily correction was 0.09‰.

4. Results

A wide range of $\delta^{18}O(Zc)$ values occur throughout the SNB. These values, grouped by geographic region, are given in Table 1. Rocks from the southern Sierra, in the Tehachapi Mts. and Lake Isabella areas, have the highest $\delta^{18}O(Zc)$ values (7.8 ± 0.7‰, $n = 42$) in the batholith (Fig. 4A). A subset of samples from the eastern Tehachapi Mts., including the Lake Isabella area, have the highest $\delta^{18}O(Zc)$ values of all (8.3 ± 0.6‰, $n = 17$). The southern Sierra samples not only lack primitive mantle values (5.3 ± 0.3‰ (1 S.D.); [39]), but also are generally much higher than the mantle, and higher than other northern, central, and foothills exposures of the batholith (6.1 ± 0.9, $n = 25$). Additional $\delta^{18}O(Zc)$ values in plutonic rocks near Sequoia National Park [40], and in the central Sierra [41] have a similar distribution to values reported herein for the central Sierra (Fig. 4B). The considerable lateral gradients of composition, age, and isotopic chemistry in the central

Notes to Table 1:
See Figs. 1 and 2 for sample locations. Latitude and longitude of sample locations and list of references for geochronology are given in Appendix A. Analysis of multiple grain-sizes of zircon for a sample are indicated by ditto (″) marks. Precision of analyses, standard deviation (S.D.), is one-half the difference between duplicate analyses. For samples analyzed only once, precision is estimated from the standard deviation of UWG-2 analyzed the same day. Values of $\delta^{18}O$ for metamorphic garnet in three samples are: 7.34 (PC36); 7.37 (PC129); 5.05 (WR91A).
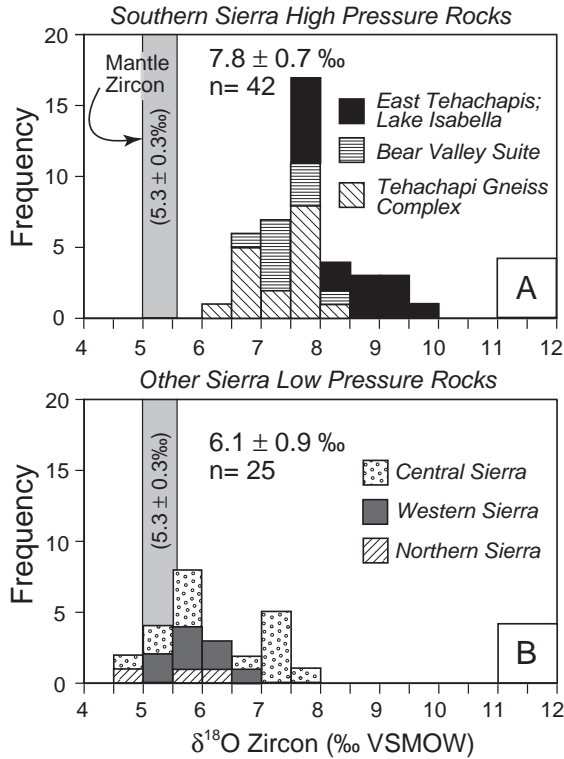
Fig. 4. Histograms of $\delta^{18}O$ for Cretaceous igneous zircons in the Sierra Nevada batholith. Values of $\delta^{18}O(Zc)$ are elevated in high pressure rocks of the southern Sierra (A), relative to volcanic and plutonic values in the rest of the batholith (B), many of which are only mildly elevated relative to the mantle value $(5.3 \pm 0.3‰)$ of Valley et al. [39].

SNB are also reflected in a wide range (3.5‰) of $\delta^{18}O(Zc)$; however, higher $\delta^{18}O$ values in the southern SNB and a wider range (4‰) indicates a larger gradient in $\delta^{18}O$ with depth in the batholith than occurs from west to east.

In the southern Sierra there are distinct trends $\delta^{18}O(Zc)$ for each group of intrusives (Fig. 5), which correlate to age (Fig. 6A). Nearly identical $\delta^{18}O(Zc)$ values are seen in the BVS $(7.5 \pm 0.4‰,$ $n=10)$ and Tehachapi Gneiss complex $(7.4 \pm 0.6,$ $n=17)$, but the BVS rocks record increasing $\delta^{18}O$ in younger rocks of the suite (Fig. 5C). Values of $\delta^{18}O(Zc)$ from the oldest and least evolved mafic magmas of the BVS suite, the Tunis Creek/Bison Peak plutons, have a very narrow range of $\delta^{18}O(Zc)$ values (7.0–7.2‰, Figs. 5C and 6A), but highly variable $\delta^{18}O(WR)$ values (5.7–8.2‰) due to alteration

(Fig. 5B). The $\delta^{18}O(Zc)$ values emphasize how alteration of $\delta^{18}O(WR)$ can obscure important details about magmatic processes, in this case the remarkable similarity in $\delta^{18}O$ of the oldest BVS suite magmas. Differences between the Gneiss complex and BVS rocks are evident when $\delta^{18}O(Zc)$ is considered relative to
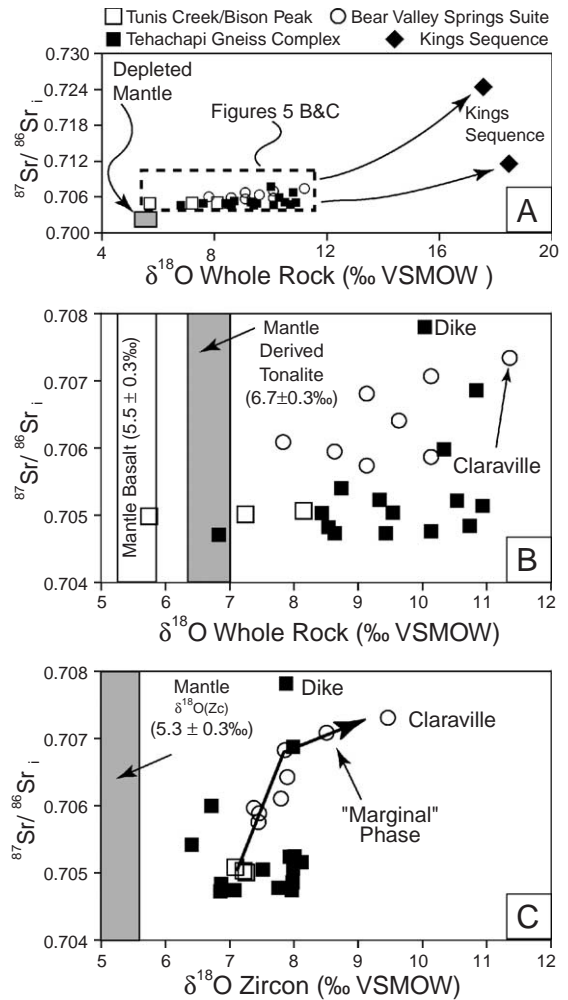

Fig. 5. Diagram of Sr_i vs. $\delta^{18}O(Zc)$ and measured $\delta^{18}O(WR)$, from [10], for the southern Sierra. (A) Compressed view shows positions of depleted mantle and the Kings Sequence relative to the BVS suite. (B) $\delta^{18}O(WR)$ vs. Sr_i for BVS suite (C) $\delta^{18}O(Zc)$ vs. Sr_i for BVS suite; black arrow in C denotes the inferred contamination path of the Bear Valley Springs tonalite as it interacted with the Kings Sequence. Note the scatter in the $\delta^{18}O(WR)$ data relative to $\delta^{18}O(Zc)$. Primitive mantle-derived basalt and tonalite $\delta^{18}O(WR)$ values are shown in B; mantle zircon value is shown in C.
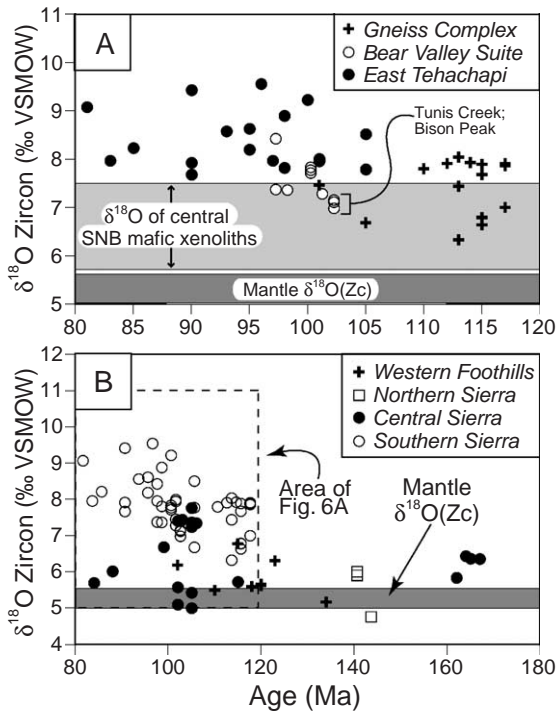
Fig. 6. Variation of $\delta^{18}O(Zc)$ with age in the Sierra Nevada. (A) In the southern Sierra, a number of the older (102–120 Ma) samples lie within a range of $\delta^{18}O$ that zircon in equilibrium with xenoliths in the Central Sierra would define. Younger rocks in the eastern Tehachapi (including Lake Isabella) lie above this field reflecting greater contamination by Kings Sequence wallrocks. (B) When all samples studied (Jurassic to Cretaceous) are considered, primitive mantle $\delta^{18}O(Zc)$ values are present throughout this time span, and younger samples record greater crustal components in the batholith with decreasing age.

Sr_i (Fig. 5B and C). The BVS suite has a clear correlation of increasing $\delta^{18}O(Zc)$ to Sr_i, with no such correlation in the Tehachapi Gneiss complex. Additionally, over time, there is more variability of $\delta^{18}O(Zc)$ throughout the SNB (Fig. 6B). This increase in the range of $\delta^{18}O$ in the SNB appears to indicate greater supracrustal input with time and is presently under investigation.

In a number of cases, different zircon grain size cohorts were analyzed for $\delta^{18}O$ to test for zoning in the grains or evidence of assimilation (Table 1). For instance, smaller zircons are often younger and would be predicted to capture a later record of contamination in magmas than older ones. Contamination by high-$\delta^{18}O$ wallrocks would thus be expected to increase

magma $\delta^{18}O$ and consequently the $\delta^{18}O$ of the youngest zircons. The variation of $\delta^{18}O$ between large and small zircons was found to be minor; the largest difference of $\delta^{18}O$ is 0.32‰ (Table 1). Moreover, younger zircons show no systematic increase in $\delta^{18}O$. The lack of significant $\delta^{18}O$ variability between grain sizes suggests individual grains lack notable zoning of $\delta^{18}O$. Thus it appears that zircon did not crystallize over long enough periods to record variable $\delta^{18}O$ due to contamination by wallrocks.

Ultramafic xenoliths from Chinese Peak have high $\delta^{18}O$ values (Table 2). The average calculated $\delta^{18}O(WR)$ of the Chinese Peak pyroxenite xenoliths is 7.24 ± 1.0‰. Pyroxene $\delta^{18}O$ fractionations, $\Delta^{18}O$(orthopyroxene–clinopyroxene), are all positive and generally small (0.3 ± 0.06‰, Table 2), except samples A and B-1, which indicates high-temperature fractionations were preserved. Also, average xenolith $\delta^{18}O(WR)$ values are essentially identical to pyroxenite xenolith values (7.2 ± 1.0‰) that Ducea (2000) [34] reported at Big Creek, a second locality in the San Joaquin volcanic field. While high $\delta^{18}O$ values were measured in granulite xenoliths at Chinese Peak [42], elevated pyroxenite $\delta^{18}O$ values confirm that high-$\delta^{18}O$ eclogitic residues were widely distributed under the central SNB.

Table 2
Chinese peak pyroxenite xenolith $\delta^{18}O$ values

Sample	$\delta^{18}O$ (Cpx)	$\delta^{18}O$ (Opx)	$\delta^{18}O$ (Phlg)	$\delta^{18}O$ (WR)[a]
1S85A	6.82 (85)	7.82 (15)		6.97
1S85B-1	5.64 (90)	6.28 (10)		5.70
1S85E	7.85 (10)	8.10 (80)	8.49 (10)	8.11
1S85E-1	7.89 (25)	8.09 (70)	8.25 (5)	8.05
1S85E-2	8.17 (90)		8.91 (10)	8.24
1S85G	5.87 (55)	6.22 (45)		6.03
1S85J-1		6.06 (85)	8.10 (15)	6.37
1S85K-2	7.93 (100)			7.93
1S85L-2	8.27 (50)	8.56 (50)		8.42
1S85M-1	7.35 (95)	7.69 (5)		7.37
1S85M-2	6.23 (90)		8.32 (10)	6.44
Average:				7.24 ± 1.0

[a] Whole rock (WR) $\delta^{18}O$ values are calculated for each xenolith based on the $\delta^{18}O$ of the phases analyzed and their approximate modal abundance, in parentheses. Samples were collected at the toe of a trachybasalt flow east of Chinese Peak (37°13′05″N, 119°09′04″W). Cpx=clinopyroxene; Opx=orthopyroxene; Phlg= phlogopite.

5. Discussion

5.1. High-$\delta^{18}O$ source rocks

Values of $\delta^{18}O(Zc)$ in both the Tehachapi Gneiss complex and BVS intrusive suite are considerably higher than uncontaminated mantle values. However most of these rocks have relatively low Sr_i (<0.705) and high εNd (>0) values, indicating they contain less than 15% of Proterozoic basement or sediments thereof [10,11]. The combination of the high $\delta^{18}O$, low Sr_i and high εNd values, especially in BVS rocks requires: (1) input of material into the source that was previously altered and had its $\delta^{18}O$ reset (raised) at or near Earth's surface during exchange with low temperature (<300 °C) hydrothermal fluids; (2) that the same material was mantle-derived and relatively young (Phanerozoic) at the time of contamination, which explains why it has relatively non-radiogenic isotope ratios. Rocks that meet these criteria include the upper portions of oceanic crust that are hydrothermally altered at spreading ridges [43,44]. This includes serpentinized peridotite, which is common along large transform faults and slow spreading ridges, as well as subduction complexes [45]. Other possible rocks include hydrothermally altered submarine volcanic arc rocks and derivative turbidite sequences [46].

Wallrock exposures of accreted oceanic lithosphere and associated cover strata in the western SNB [47], are possible candidates or remnants of the high-$\delta^{18}O$ source. In the western Sierra, serpentinized peridotite massifs and bounding serpentinite-matrix ocean floor mélange belts derived from Paleozoic abyssal lithosphere constitute an extensive basement complex. Thick Paleozoic to lower Mesozoic hemipelagic deposits are associated with the basement complex, and are themselves overlain by thinner lower Mesozoic submarine volcanic arc and turbiditic strata. These rocks are sutured to the North American crust along a truncation zone that cut obliquely across the North American passive margin; juxtaposition entailed a combination of transform faulting and subduction.

Subduction or underthrusting of such rocks could have delivered them to the base of Sierran arc where they were incorporated into magmas. Once subducted, the high $\delta^{18}O$ signature of these rocks was conveyed to magmas in the lower crust of the SNB by fluids and hydrous silicate melts. Isotope and trace element studies of modern arcs indicate that fluids and melts released from oceanic crust, mostly from hydrated upper parts and overlying sediments, initiate melting in the sub-arc mantle, which forms hydrous silicate melts that ultimately enter the base of the arc [48].

5.2. Quantifying supracrustal input

Oxygen isotopes provide a basis for estimating a minimum quantity of crust incorporated by the deep SNB. Mass balance calculations can be made assuming magmas and contaminant fluids/melts contain equal amounts of oxygen (~50 wt.%), that initial $\delta^{18}O(WR)$ was 5.7‰ (mantle value), and final $\delta^{18}O(WR)$ was in equilibrium with measured $\delta^{18}O(Zc)$ values.

The values of $\delta^{18}O(WR)$ in equilibrium with $\delta^{18}O(Zc)$ can be calculated. This is possible using the recognized relationship that increasing SiO_2 results in an increasing *proportion* of felsic, high-$\delta^{18}O$ minerals in a granitic rock, which increases $\delta^{18}O(WR)$ regularly during fractional crystallization [13]. Values of $\Delta^{18}O$ (WR−Zc) will change at approximately the same rate as $\delta^{18}O(WR)$ assuming all minerals and melt exchange oxygen and are in equilibrium. Since equilibrium fractionation between minerals changes minimally over the temperature ranges encountered during crystallization of a magma, the effect of temperature in calculating $\delta^{18}O(WR)$ is very small [13]. As an approximation, $\Delta^{18}O(WR–Zc)$ can be related to the weight percentage of SiO_2. As shown by Valley et al. (1994) [49] rocks ranging in composition from gabbro and granite have approximately linear dependence of $\Delta^{18}O(WR–Zc)$, such that $\delta^{18}O(WR) \approx 0.06(wt.\% \ SiO_2) - 2.25 + {}^{18}O(Zc)$. For a worked example, the $\delta^{18}O(Zc)$ value of the Tunis Creek gabbro (7.0‰) yields a calculated $\delta^{18}O(WR)$ of 7.4‰ for its 45% SiO_2. It follows that increasing a typical uncontaminated mantle value (5.7‰) to the value calculated of the Tunis Creek gabbro requires minimum supracrustal additions of 18% of altered oceanic crust ($\delta^{18}O(WR)=15‰$), or 27% of greywacke ($\delta^{18}O(WR)=12‰$).

To determine if observed $\delta^{18}O$–Sr_i trends (Fig. 5) could be accounted for by mixing of melts with upper mantle compositions with melts from Kings Sequence metasedimentary rocks (Fig. 5A), both bulk mixing

and assimilation-fractional-crystallization (AFC) [50] scenarios were conducted. Modeling reveals unrealistic amounts of assimilation and unrealistic solid–liquid Sr partitioning values are required to reproduce the measured $\delta^{18}O$ and Sr_i values of the Tunis Creek gabbro. However, $\delta^{18}O$ vs. Sr_i values can be reasonably reproduced by mixing melts of primitive upper mantle and altered ocean crust. Additionally, both bulk and AFC modeling of modest input (8–12%) of Kings Sequence rocks into the Tunis Creek gabbro or Bison Peak tonalite reproduces the $\delta^{18}O$–Sr_i trend seen in the Bear Valley Springs tonalite (Fig. 5B and C). Collectively, the modeling suggests the parent magmas (i.e., the Tunis Creek gabbro) of the BVS suite had a high $\delta^{18}O$ source. Ascent of these magmas into the base of the arc then allowed contamination by the Kings Sequence, producing the Bear Valley Springs tonalite. As described earlier, patterns of Proterozoic zircon U/Pb inheritance in the BVS are also consistent with progressively greater contamination by the Kings Sequence in the younger and shallower rocks, like those in the eastern Tehachapis (Fig. 6A). The elevated $\delta^{18}O(Zc)$ and Sr_i values of these rocks indicate such contamination, and approach values of the highly contaminated granodiorite of Claraville and other small granite and leucogranite bodies in the eastern Tehachapis, which show a clear trend toward higher $\delta^{18}O$ with younger age (Fig. 6A).

5.3. Timing and distribution of supracrustal input

The age of the supracrustal rocks is older and more variable, as is the timing of their emplacement, than the resultant high-$\delta^{18}O$ granitic rocks. As described earlier, pronounced chemical and compositional gradients across the batholith reflect the different source characteristics of juxtaposed Phanerozoic and Proterozoic lithospheres. Because accretion of oceanic terranes occurred in the Paleozoic, the timing of delivery of the supracrustal rocks beneath the SNB arc is Paleozoic to Mesozoic in age.

The fate of accreted Paleozoic or Mesozoic oceanic terranes relative to the arcs under which they were subducted/emplaced is uncertain. Conceivably these terranes contributed to the formation of magmas that migrated into or underplated the then active arc; they may also have contaminated the sub-arc lithospheric

mantle (Fig. 7A); or both processes may have occurred.

Regardless of the early fate of these subducted rocks, the onset of voluminous Cretaceous magmatism reconstituted the entire crustal column in the Sierran arc [30,31]. Reconstitution of crustal rocks is inferred to have occurred in the MASH zone beneath the arc (Fig. 7B). As homogenized felsic magmas were emplaced in the middle and upper crust above the MASH zone, eclogitic residues were expelled below it and would eventually form the root of the batholith (Fig. 7B). Abundant Proterozoic sediments were deposited at the edge of North America before the batholith formed, however these sedimentary rocks would be expected to be incorporated into magmas in and above the MASH zone. Melting of such rocks in the MASH zone requires considerable downward wallrock transport [30,31], or lithospheric-scale thrusting (Fig. 7B) beneath the arc [51]. In the eastern Sierra, significant volumes of granitic crust were generated directly from enriched Proterozoic lithospheric mantle (Fig. 7B), which was undisturbed until a sufficiently large magmatic event in the Cretaceous led to massive melting and magma generation [25,51]. Preconditioning of the lithospheric mantle before the Cretaceous likely occurred in the western SNB, and the lithospheric mantle there stored Phanerozoic rocks.

Central SNB xenoliths provide insight about the vertical distribution of Proterozoic versus Phanerozoic supracrustal rock beneath the arc. The two groups of Cretaceous age xenoliths in the central Sierra have distinct isotope ratios as shown by this and other studies [34,42,52]. Felsic, granulitic xenoliths have elevated Sr_i values (>0.707), and most have high $\delta^{18}O(WR)$ values (9–14‰). Such isotope patterns indicate that the granulitic xenoliths contain a large component of crust or sedimentary rocks of Proterozoic age. In contrast, mafic, eclogitic xenoliths have Sr_i values (0.7051–0.7062) consistent with Pre-Cretaceous supracrustal input, but their elevated $\delta^{18}O(WR)$ values (7–9‰, Table 2) are 1–2‰ greater than would be expected of Proterozoic supracrustal rocks with the same Sr_i. Furthermore, $\delta^{18}O$ and Sr_i for the two xenolith suites show distinct correlations for each suite [42]. The $\delta^{18}O$ vs. Sr_i trend in the pyroxenite suite can be reproduced as a mixture of Phanerozoic supracrustal material and depleted mantle.
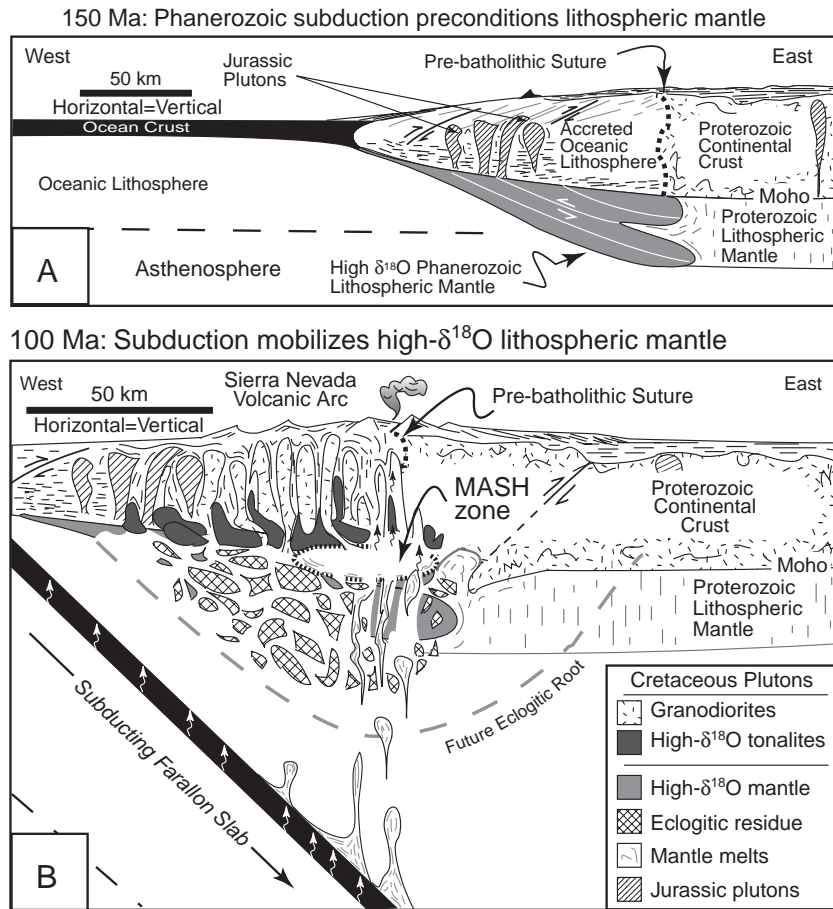
Fig. 7. Proposed model to produce the high-δ^{18}O intrusives in the deep crust of the Sierra Nevada. (A) At 150 Ma, the lithospheric mantle beneath the SNB contains Mesozoic to Paleozoic altered ocean crust and similar high-δ^{18}O rock that was subducted and/or underthrust beneath the arc sometime in the Paleozoic to Jurassic. Note the pre-batholithic suture between accreted oceanic crust and North American continental crust. (B) At 100 Ma, magmatic activity has fully mobilized the high-δ^{18}O lithospheric mantle producing a stratification of δ^{18}O, with high-δ^{18}O tonalitic magmas at depth in the SNB. "Future eclogitic root" refers to the lowermost extent of eclogitic residues expelled from the MASH zone when magmatic activity ceased in the Late Cretaceous. Modified after [31].

Notably, the pyroxenite xenolith Sr_i and δ^{18}O(WR) values overlap remarkably with gabbros of the Bear Valley Springs suite. The ϵNd values of the two xenolith suites overlap, suggesting homogenization of Nd isotope ratios during magma genesis in the lower crust and sub-arc mantle, and possibly involvement of aged lithospheric mantle (e.g., [25]). From a mass balance point of view, pyroxenite xenoliths appear representative of the batholithic root between 40 and 70 km depth [31] (Fig. 7B), which suggests ~20% of the arc's supracrustal δ^{18}O signature is Phanerozoic.

5.4. High-δ^{18}O rocks and the 0.706 line

The general correspondence of the $Sr_i = 0.706$ isopleth to the pre-batholithic suture between accreted oceanic lithosphere and North American lithosphere has been well established by both geochemical and geologic studies (cf. [4,47]). Recognizing that some of the highest δ^{18}O values measured in the SNB are from rocks with <0.706 Sr_i values is particularly important, because it proves that those rocks were not primitive and derived solely from mantle sources. High-δ^{18}O rocks with <0.706 Sr_i values in the SNB are in fact

prevalent. Beside deep crustal exposures of high-δ^{18}O tonalitic magmas in the southern SNB, a number of high δ^{18}O values are reported for tonalites and diorites in the western SNB near Sequoia National Park [40]. Other high δ^{18}O values are found in the Bass Lake tonalite [41], west of Yosemite National Park. The Bass Lake tonalite has a large area similar to that of the Bear Valley Springs tonalite, and it appears to have relatively deep igneous crystallization pressures (>4 kbar [26]) like the Bear Valley Springs tonalite. The similarity of these tonalites is intriguing and suggests they have similar origins. At the least, the tonalites' large areas (>1000 km^2 each) shows that supracrustal recycling occurred on a large scale.

5.5. Processes of crust formation in the Sierra Nevada

The site of supracrustal additions to SNB magmas sheds considerable light on the processes of crust formation in the batholith. In particular, the high δ^{18}O(Zc) values in Tehachapi diorites and tonalites require that supracrustal rocks were added to SNB magmas in the lower crust and below, in a MASH zone (Fig. 7B). The geophysical structure of the Sierra Nevada indicates that the Tehachapis are probably representative of the deep crust throughout the batholith [53]. If the high pressure rocks of the southern Sierra are representative of the deep crust of the entire batholith, then it is likely that large amounts of high-δ^{18}O material were added to magmas at depth throughout the Sierran arc. Granitoids found in the Salinian block of west-central California, a displaced part of the Sierran arc, also have high δ^{18}O values [9], which further indicates widespread high-δ^{18}O input. The high δ^{18}O Bass Lake tonalite in the central SNB hints at such continuity. High-δ^{18}O xenoliths in the central Sierra extend the region of supracrustal addition downward. Pyroxenite xenoliths, including some from up to 70 km beneath the arc [54], confirm that high-δ^{18}O material extended to much greater depths than the limit of the lower crust of a significant part of the eclogitic root of the batholith (Fig. 7).

While the geochemistry of most plutons in the SNB reflects processes occurring in the lithospheric mantle and lower crustal sources, contamination by Proterozoic metasedimentary rocks is detectable in small granite plutons of the younger eastern Tehachapis (Fig. 2). Detailed study of some of these plutons indicates that their radiogenic isotopic heterogeneity is a function of deeper sources, but that they have detectable contamination proximal to thin migmatite zones that border them [37]. Garnet bearing, peraluminous granites in the central SNB also record oxygen isotope evidence of contamination, at scales of meters to tens of meters, at their margins [55,56]. The highly evolved chemistry of the peraluminous plutons seems largely to be a lower crustal feature, with superimposed middle and upper crust contamination. For instance, while δ^{18}O(Zc) values of peraluminous granitoids are high (7.5–8.0‰) throughout, Sr$_i$ values in these plutons are relatively low (0.704–0.707), except at their margins. Therefore their isotope patterns are not consistent with abundant input of Kings Sequence metasediments; instead they likely were generated from sources like that proposed for rocks in this study.

It is intriguing that δ^{18}O(Zc) values vary with depth in the batholith (Fig. 4A). This "stratification" of δ^{18}O suggests that assimilation of supracrustal rocks was more efficient at depth, and resulted in formation of large, high-δ^{18}O tonalitic magmas like the Bear Valley Springs and Bass Lake tonalites. These plutons seem to have stalled in the lower crust, presumably due to density filtering, just above the arc's MASH zone (Fig. 7B). Greater numbers of felsic plutons above the MASH zone suggest that mafic and felsic magmas were emplaced separately in some cases and that the felsic magmas were capable of rising higher into the crust. While a MASH zone would be expected to homogenize δ^{18}O values in the mafic and felsic granites, it is possible that tonalitic magmas were precursors that effectively "purged" the lithospheric mantle of Phanerozoic high-δ^{18}O material (Fig. 7A). This may have allowed later magmas to form with more mantle-like δ^{18}O values. Potentially this δ^{18}O stratification extends throughout the entire SNB. Such stratification is the subject of ongoing research. Regardless of its distribution, vertical stratification begs revision of models for convergent margin magmatism based on two-dimensional geochemical gradients.

We note that globally, mafic lower crust has been shown to have a high average δ^{18}O in many cases [49,57–61]. This suggests that addition of high-δ^{18}O material to mafic magmas in the lower continental crust is common. Recognition of this process may be obscured in many cases due to post-magmatic alteration or simply due to a lack of sufficient expo-

sures of deep crustal rocks, which generally is the case in modern convergent margin batholiths.

6. Conclusions

Oxygen isotopes show that granitoids from exposed high-pressure rocks in the southern Sierra Nevada contain a significant portion, at least 18% by mass, of supracrustal material. The supracrustal component was young mantle-derived rock that was hydrothermally altered and then subducted beneath the arc in the Mesozoic or Paleozoic. Additional contamination (8–12%) of such magmas occurred by interaction with the Kings Sequence in the upper parts of the batholith. Vigorous magmatism in the Cretaceous melted these rocks and relayed the supracrustal signature to magmas in the base of the batholith and above. The presence of high-δ^{18}O values in xenoliths confirms that supracrustal rocks were present in the sub-arc lithospheric mantle. These findings indicate that additions of high-δ^{18}O material to the lower crust may be significant in convergent, continental margin arcs through recycling of young, mantle-derived material. Recognizing these contributions has been hindered by non-exposure of the roots of convergent margin batholiths, vertical geochemical gradients, and interaction with overlying continental crust.

Appendix A. Supplementary data

Supplementary data associated with this article can be found, in the online version, at doi:10.1016/ j.epsl.2005.04.003.

References

[1] A. Reymer, G. Schubert, Phanerozoic addition rates to the continental crust and crustal growth, Tectonics 3 (1984) 63–77.

[2] J. Tarney, C.E. Jones, Trace element geochemistry of orogenic igneous rocks and crustal growth models, J. Geol. Soc. (Lond.) 151 (1994) 855–868.

[3] R.L. Rudnick, Making continental crust, Nature 378 (1995) 571–578.

[4] R.W. Kistler, Two different lithosphere types in the Sierra Nevada, California, in: L. Anderson (Ed.), The Nature and Origin of Cordilleran Magmatism, Memoir-Geological Society Of America (GSA), vol. 174, Geological Society of America, Boulder, CO, United States, 1990, pp. 271–281.

[5] C.W. Jennings, R.G. Strand, T.H. Rogers, Geologic map of California (1977) 1 sheet, 1:750,000.

[6] J.G. Moore, T.W. Sisson, Preliminary geologic map of Sequoia and Kings Canyon national parks, California, U.S. Geol. Surv. Open File Rep. 87-0651 (1987) 1 sheet 1:125,000, 17 pp.

[7] M.T. McCulloch, R.T. Gregory, G.J. Wasserburg, H.P. Taylor, A neodymium, strontium, and oxygen isotope study of the Cretaceous Samail Ophiolite and implications for the petrogenesis and seawater-hydrothermal alteration of oceanic crust, Earth Planet. Sci. Lett. 46 (1980) 201–211.

[8] H.P. Taylor, L.T. Silver, Oxygen isotope relationships in plutonic igneous rocks of the Peninsular Ranges Batholith, southern and Baja California, Open-File Rep. (U. S. Geol. Surv.) 78-0701 (1978) 423–426.

[9] U. Masi, J.R. O'Neil, R.W. Kistler, Stable isotope systematics in mesozoic granites of central and northern California and southwestern Oregon, Contrib. Mineral. Petrol. 76 (1981) 116–126.

[10] J.B. Saleeby, D.B. Sams, R.W. Kistler, U/Pb zircon, strontium, and oxygen isotopic and geochronological study of the southernmost Sierra Nevada Batholith, California, J. Geophys. Res. 92 (1987) 10,443–10,466.

[11] D.A. Pickett, J.B. Saleeby, Nd, Sr, and Pb isotopic characteristics of Cretaceous intrusive rocks from deep levels of the Sierra Nevada Batholith, Tehachapi Mountains, California, Contrib. Mineral. Petrol. 118 (1994) 198–215.

[12] D.J. Wood, J.B. Saleeby, Late cretaceous–paleocene extensional collapse and disaggregation of the southernmost Sierra Nevada Batholith, Int. Geol. Rev. 39 (1997) 973–1009.

[13] J.W. Valley, Oxygen isotopes in zircon, in: J.M. Hanchar, P.W.O. Hoskin (Eds.), Zircon, Min. Soc. Am. Rev. in Mineral. Geochem., vol. 53, 2003, pp. 343–385.

[14] D.C. Ross, Generalized geologic map of the southern Sierra Nevada, California, showing the location of basement samples for which whole rock ^{18}O has been determined, U.S, Geol. Surv. Open-File Rep. 83-0904 1 sheet, 1:250,000 (1983).

[15] J.G. Moore, The quartz diorite boundary line in the western United States, J. Geol. 67 (1959) 198–210.

[16] P.C. Bateman, Plutonism in the central part of the Sierra Nevada Batholith, California, Prof. Pap.-Geol. Surv. (U. S.) 1483 (1992) (186 pp.).

[17] R.W. Kistler, Z.E. Peterman, Variations in Sr, Rb, K, Na, and initial Sr^{87}/Sr^{86} in mesozoic granitic rocks and intruded wall

rocks in central California, Geol. Soc. Amer. Bull. 84 (1973) 3489–3512.

[18] R.W. Kistler, Z.E. Peterman, Reconstruction of crustal blocks of California on the basis of initial strontium isotopic compositions of mesozoic granitic rocks, Prof. Pap.-Geol. Surv. (U. S.) 1071 (1978) (17 pp.).

[19] T.W. Stern, P.C. Bateman, B.A. Morgan, M.F. Newell, D.L. Peck, Isotopic U–Pb ages of zircon from the granitoids of the central Sierra Nevada, California, Prof. Pap.-Geol. Surv. (U. S.) 1185 (1981) 17.

[20] J.H. Chen, J.G. Moore, Uranium–lead isotopic ages from the Sierra Nevada batholith, California, J. Geophys. Res. 87 (1982) 4761–4784.

[21] J.J. Ague, G.H. Brimhall, Regional variations in bulk chemistry, mineralogy, and the compositions of mafic and accessory minerals in the batholiths of California: with Suppl. Data 88-13, Geol. Soc. Amer. Bull. 100 (1988) 891–911.

[22] R.W. Kistler, Mesozoic intrabatholithic faulting, Sierra Nevada, California, in: G. Dunne, K. McDougall (Eds.), Mesozoic Paleography of the Western United States II, Pacific Section SEPM, vol. 71, 1994, pp. 247–262.

[23] D.J. DePaolo, A neodymium and strontium isotopic study of the Mesozoic calc-alkaline granitic batholiths of the Sierra Nevada and Peninsular Ranges, California, JGR. J. Geophys. Res. 86 (1981) 10470–10488.

[24] J.H. Chen, G.R. Tilton, Applications of lead and strontium isotopic relationships to the petrogenesis of granitoid rocks, central Sierra Nevada batholith, California, Geol. Soc. Amer. Bull. 103 (1991) 437–447.

[25] D.S. Coleman, A.F. Glazner, The Sierra Crest magmatic event: rapid formation of juvenile crust during the Late Cretaceous in California, Int. Geol. Rev. 39 (1997) 768–787.

[26] J.J. Ague, G.H. Brimhall, Magmatic arc asymmetry and distribution of anomalous plutonic belts in the batholiths of California: effects of assimilation, crustal thickness, and depth of crystallization, Geol. Soc. Amer. Bull. 100 (1988) 912–927.

[27] J.J. Ague, Thermodynamic calculation of emplacement pressures for batholithic rocks, California: implications for the aluminum-in-hornblende barometer, Geology 25 (1997) 563–566.

[28] D.A. Pickett, J.B. Saleeby, Thermobarometric constraints on the depth of the exposure and conditions of plutonism and metamorphism at deep levels of the Sierra Nevada batholith, Tehachapi Mountains, California, J. Geophys. Res. 98 (1993) 609–629.

[29] E.T. Dixon, E.J. Essene, A.N. Halliday, Critical tests of hornblende barometry, Lake Isabella to Tehachapi area, southern Sierra Nevada, California, Eos. Trans.-Am. Geophys. Union 75 (1994) 744.

[30] J.B. Saleeby, Progress in tectonic and petrogenetic studies in an exposed cross-section of young (~100 Ma) continental crust, southern Sierra Nevada, California, in: M.H. Salisbury, D.M. Fountain (Eds.), Exposed Cross-Sections of the Continental Crust, NATO ASI Series, vol. 317 C, D. Reidel, Dordrecht, 1990, pp. 137–158.

[31] J. Saleeby, M. Ducea, D. Clemens Knott, Production and loss of high-density batholithic root, southern Sierra Nevada, California, Tectonics 22 (2003), doi:10.1029/2002TC001374.

[32] P.E. Malin, E.D. Goodman, T.L. Henyey, Y.G. Li, D.A. Okaya, J.B. Saleeby, Significance of seismic reflections beneath a tilted exposure of deep continental crust, Tehachapi Mountains, California, J. Geophys. Res. 100 (1995) 2069–2087.

[33] W. Hildreth, S. Moorbath, Crustal contributions to arc magmatism in the Andes of central Chile, Contrib. Mineral. Petrol. 98 (1988) 455–489.

[34] M. Ducea, Constraints on the bulk composition and root foundering rates of continental arcs: a California arc perspective, J. Geophys. Res. 107 (2002) ECV 15.1–ECV 15.13.

[35] D.B. Sams, J.B. Saleeby, Geology and petrotectonic significance of crystalline rocks of the southernmost Sierra Nevada, California, in: W.G. Ernst (Ed.), Metamorphism and Crustal Evolution of the Western United States, Rubey Volume, Prentice-Hall, Englewood Cliffs, 1988, pp. 865–893.

[36] J.B. Saleeby, C. Busby-Spera, Fieldtrip guide to the metamorphic framework rocks of the Lake Isabella area, southern Sierra Nevada, California, in: G. Dunne (Ed.), Mesozoic and Cenozoic Structural Evolution of Selected Areas, East-Central California, Geol. Soc. Am., Cordilleran Sect., Los Angeles, 1986, pp. 81–94.

[37] L. Zeng, Non-modal partial melting of metasedimentary pendants in the southern Sierra Nevada and implications for the deep origin of within-pluton isotopic heterogeneity, PhD thesis, California Institute of Technology, Pasadena, CA (2003).

[38] J.W. Valley, N. Kitchen, M.J. Kohn, C.R. Niendorf, M.J. Spicuzza, UWG-2, a garnet standard for oxygen isotope ratios: strategies for high precision and accuracy with laser heating, Geochim. Cosmochim. Acta 59 (1995) 5223–5231.

[39] J.W. Valley, P.D. Kinny, D.J. Schulze, M.J. Spicuzza, Zircon megacrysts from kimberlite: oxygen isotope variability among mantle melts, Contrib. Mineral. Petrol. 133 (1998) 1–11.

[40] J.S. Lackey, J.W. Valley, J.H. Chen, Correlated O–Sr–Pb isotope ratios in the West-Central Sierra Nevada batholith, California, Abstr. Programs-Geol. Soc. Am. 33 (2001) 295.

[41] J.S. Lackey, J.W. Valley, D.F. Stockli, M.A. House, Magmatic processes in the central Sierra Nevada batholith: a cryptic pre-Jurassic boundary in Long Valley, California, Abstr. Programs-Geol. Soc. Am. 35 (2003) 92.

[42] M.N. Ducea, A petrologic investigation of deep-crustal and upper-mantle xenoliths from the Sierra Nevada, California: constraints on lithospheric composition beneath continental arcs and the origin of Cordilleran batholiths, PhD thesis, California Institute of Technology, Pasadena (1998).

[43] K. Muehlenbachs, Alteration of the oceanic crust and the ^{18}O history of seawater, in: J.W. Valley, H.P. Taylor Jr., J.R. O'Neil (Eds.), Stable Isotopes in High Temperature Geological Processes, Min. Soc. Am. Rev. Mineral., vol. 16, 1986, pp. 425–444.

[44] K. Muehlenbachs, The oxygen isotopic composition of the oceans, sediments and the seafloor, Chem. Geol. 145 (1998) 263–273.

[45] J.B. Saleeby, Tectonic significance of serpentinite mobility and ophiolitic melange, in: L.A. Ramond (Ed.), Melanges—their

Nature, Origin and Significance, Spec. Pap.-Geol. Soc. Am., vol. 198, 1984, pp. 153–168.

[46] M. Magaritz, H.P. Taylor Jr., Oxygen, hydrogen and carbon isotope studies of the Franciscan Formation, Coast Ranges, California, Geochim. Cosmochim. Acta 40 (1976) 215–234.

[47] J.B. Saleeby, Petrotectonic and paleogeographic settings of U.S. Cordilleran ophiolites, in: B.C. Burchfiel, P.W. Lipman, M.L. Zoback (Eds.), The Cordilleran Orogen: Conterminous U.S.: The Geology of North America, Geol. Soc. Am., G-3, Boulder, 1992, pp. 653–682.

[48] R.J. Stern, Subduction zones, Rev. Geophys. 4 (2002) 3-1 to 3-38.

[49] J.W. Valley, J.R. Chiarenzelli, J.M. McLelland, Oxygen isotope geochemistry of zircon, Earth Planet. Sci. Lett. 126 (1994) 187–206.

[50] D.J. DePaolo, Trace element and isotopic effects of combined wallrock assimilation and fractional crystallization, Earth Planet. Sci. Lett. 53 (1981) 189–202.

[51] M. Ducea, The California Arc: thick granitic batholiths, eclogitic residues, lithospheric-scale thrusting, and magmatic flare-ups, GSA Today 11 (2001) 4–10.

[52] D. Clemens-Knott, Neodymium isotope constraints on the character of the central Sierra Nevada deep crust and upper mantle: Chinese Peak xenoliths, Abstr. Programs-Geol. Soc. Am. 28 (1996) 56.

[53] M.M. Fliedner, S.L. Klemperer, N.I. Christensen, Three-dimensional seismic model of the Sierra Nevada Arc, California, and its implications for crustal and upper mantle composition, J. Geophys. Res. 105 (2000) 10899–10921.

[54] M.N. Ducea, J.B. Saleeby, The age and origin of a thick mafic–ultramafic keel from beneath the Sierra Nevada Batholith, Contrib. Mineral. Petrol. 133 (1998) 169–185.

[55] H.J. Hinke, J.S. Lackey, J.W. Valley, Oxygen isotope record of magmatic evolution: the garnet-bearing Dinkey Dome pluton, Sierra Nevada, Abstr. Programs-Geol. Soc. Am. 34 (2002) 270.

[56] J.S. Lackey, H.J. Hinke, J.W. Valley, Tracking contamination in felsic magma chambers with $\delta^{18}O$ of magmatic garnet and zircon, V. M. Goldschmidt conference: extended abstracts, Geochim. Cosmochim. Acta 66 (Suppl. 1) (2002) 428.

[57] J.W. Valley, S.R. Bohlen, E.J. Essene, W. Lamb, Metamorphism in the Adirondacks: II. the role of fluids, J. Petrol. 31 (1990) 555–596.

[58] P.D. Kempton, R.S. Harmon, Oxygen isotope evidence for large-scale hybridization of the lower crust during magmatic underplating, Geochim. Cosmochim. Acta 56 (1992) 971–986.

[59] H. Li, H. Schwarcz, D.M. Shaw, Deep crustal oxygen isotope variations: the Wawa–Kapuskasing crustal transect, Ontario, Contrib. Mineral. Petrol. 107 (1991) 448–458.

[60] J.M. Eiler, J.W. Valley, Preservation of premetamorphic oxygen isotope ratios in granitic orthogneiss from the Adirondack Mountains, New York, USA, Geochim. Cosmochim. Acta 58 (1994) 5525–5535.

[61] W.H. Peck, J.W. Valley, Large crustal input to high $\delta^{18}O$ anorthosite massifs of the southern Grenville Province: new evidence from the Morin Complex, Quebec, Contrib. Mineral. Petrol. 139 (2000) 402–417.